Application of the Optical Flow Method to Velocity Determination in Hydraulic Structure Models

D. B. Bung
bung@fh-aachen.de

Daniel Valero
valero@fh-aachen.de

6th International Symposium on Hydraulic Structures Portland, Oregon, USA, 27-30 June 2016
Hydraulic Structures and Water System Management
ISBN 978-1-884575-75-4 DOI: 10.15142/T3150628160853

Application of the Optical Flow Method to Velocity Determination in Hydraulic Structure Models

D.B. Bung[1] and D. Valero[1,2]
[1]Hydraulic Engineering Section, Civil Engineering Department
FH Aachen University of Applied Sciences
Bayernallee 9, 52066 Aachen
Germany
[2]Dept. of ArGEnCo, Univ. of Liege (ULg)
Research Group of Hydraulics in Environmental and Civil Engineering (HECE)
Chemin des Chevreuils 1, 4000 Liège
Belgium
E-mail: bung@fh-aachen.de

ABSTRACT

Optical flow estimation is used in Computer Vision for detection of moving obstacles in a sequence of images. The optical flow (OF) is defined as the displacement of brightness patterns between two sequent images. In this paper, this method is applied to high-speed images taken in hydraulic structure models for determination of velocity fields. Water is seeded with tracer particles in two cases and is self-aerated in a third case. It will be shown that the OF method gives valuable results that compare well to other velocity measurements, e.g. by Particle Image Velocimetry. The OF method is generally more time-consuming compared to PIV, but an advantage is given by the density of information when using a so-called global method, as velocity information is obtained at every pixel location.

Keywords: *Optical flow, particle image velocimetry, imaging techniques, velocity estimation.*

1. INTRODUCTION

Physical modeling of hydraulic structures is still a common technique to elaborate flow patterns, water depths, flow velocities, turbulence, etc. Flow velocities are typically measured by means of intrusive probes, such as anemometers for 1D and ADVs for 3D point measuring in clear water (ASCE 2000) and dual-tip conductivity or fiber-optical probes in bubbly flows (Felder and Chanson 2015). A drawback of these probes is the limitation to a single point, i.e. the velocity is obtained as a local value and the inevitable perturbation of the flow.

If one is interested in instantaneous 2D (or 3D) flow fields, Particle Image Velocimetry (PIV) is a widely accepted technique based on cross-correlation of subsequent frames from a video, which is captured with either a standard or high-speed camera depending on the expected flow velocity (Adrian and Westerweel 2011). To visualize the flow, a tracer material needs to be added to the water. Subsequent frames are divided into so-called interrogation windows of user-defined sizes and 2D cross-correlation in spatial or frequency domain is performed to find the most probable displacements of particles within these windows by using different peak finding methods. The method is thus an integral approach yielding a single statistically determined velocity information for each interrogation window.

Another imaging technique which may be applied to experimental fluid mechanics is given by the Optical Flow method (OF). Coming from computer vision field, it is not yet well-known in the community. To date, this method is mainly used in fields like video compression (motion estimation to predict intermediate frames) or vehicle navigation (autonomous car driving) as reported by Fortun et al. (2015). A first approach for optical flow estimation was presented by Horn and Schunck (1981), defining the optical flow as the movement of brightness (intensity) patterns in a sequence of images. OF aims to approximate a 2D motion or velocity field, which is a projection of generally 3D velocities of surface points onto the imaging surface from spatiotemporal patterns of image intensity. In order to relate the movement of brightness patterns to the movement of an object, it is assumed that the brightness of a moving pixel in the pattern remains constant during the movement. The Horn and Schunck method is a global

method attempting to minimize a global energy function. In addition, local methods have been developed based on optimization of local energy-like expression. For instance, Lucas and Kanade (1981) assume a small, constant optical flow within a neighborhood. By consequence, this method does not allow the determination of optical flow within a region of uniform intensity. Local methods can only provide sparse flow fields in contrast to global methods, which provide dense flow fields with velocity information at every point. Since its original formulation, several improvements and further developments on this basic idea of the optical flow method have been presented and give surprisingly good results although the basic assumption of brightness constancy may be unrealistic in many applications due to shading effects or changes in illumination.

In some recent studies, the Horn and Schunck approach was applied to fluid flows using particle images obtained from PIV measurements (Liu et al. 2015; Liu and Shen 2008). Corpetti et al. (2006) confirm a good agreement with PIV data implementing an approach to account for the continuity equation as well as divergence and vorticity structures of the flow. Liu et al. (2015) state that OF, as a differential approach, is more suitable to images with continuous patterns so that single particles used for PIV are not the best case for OF.

This paper aims to test the Optical Flow method to the field of hydraulic structures modeling for 1) clear water flows being seeded with particles and 2) aerated flows.

2. METHODODOGY

The constancy of brightness $I(X,Y,t)$ of a moving pixel with pixel coordinates X and Y at time t may be expressed as:

$$\frac{dI}{dt} = \frac{\partial I}{\partial t} + \frac{\partial I}{\partial X}\frac{\partial X}{\partial t} + \frac{\partial I}{\partial Y}\frac{\partial Y}{\partial t} = 0 \tag{1}$$

with I_t the temporal derivative, I_X and I_Y the spatial image derivatives in X and Y direction, and U and V the unknown spatial displacements in X and Y directions between two sequent frames. Eq. (1) may be rewritten as

$$I_t + I_X U + I_Y V = 0 \tag{2}$$

Eq. (2) is the spatial term. In order to solve this ill-posed problem (1 equation, 2 variables), a second constraint, i.e. a data term, is required. Horn and Schunck (1981) assumed that neighboring points have a similar velocity by reducing the square of the gradients of the optical flow velocity. Thus, the following objective function needs to be minimized:

$$E = \int\int \left[(I_X U + I_Y V + I_t)^2 + \alpha \left(|\nabla U|^2 + |\nabla V|^2 \right) \right] dX dY \tag{3}$$

where $\nabla = (\partial/\partial X, \partial/\partial Y)$ is the spatial gradient and α a smoothing factor for the spatial term. This minimization yields (Bruhn et al. 2005):

$$\alpha \Delta U - \left(I_X I_t + I_X{}^2 U + I_X I_Y V \right) = 0 \tag{4a}$$

$$\alpha \Delta U - \left(I_Y I_t + I_Y{}^2 U + I_X I_Y U \right) = 0 \tag{4b}$$

Where ΔU is the spatial Laplace operator over U defined by the scalar product $\nabla \cdot \nabla \mathrm{U}$. At image locations with low information from pixel derivatives, no reliable local flow estimate is possible. The Laplace operator fills in information from the neighborhood, α then works as a diffusion coefficient for U and V.

For this paper, an open-source MATLAB® toolbox for Optical Flow determination developed by Sun et al. (2010) is employed. This toolbox implements several different OF methods besides the classical Horn and Schunck method given above as well as different additional image processing techniques, which were developed in the recent past and known to likely improve the results. Bung and Valero (2016) showed that this toolbox can give valuable results in highly aerated flows on stepped spillways when using the air bubbles as seeding. A similar approach was introduced by Ryu et al. (2005) and applied by Bung (2011b), Leandro et al. (2014), and Bung and Valero (2015) using the Bubble Image Velocimetry (BIV) technique, an adapted Particle Image Velocimetry (PIV) technique using the bubbles instead of tracer particles. In order to demonstrate the general applicability of OF to water flows around hydraulic structures, all investigations are limited to the basic Horn and Schunck scheme.

In detail, three test cases are investigated:

1. Dam-break flow being observed in a 30 cm wide flume with an initial water depth of 40 cm in the reservoir (images taken from Oertel and Bung 2012); images of the seeded flow are taken with a high-speed camera at 900 fps and 1280 x 576 px resolution; the OF method is compared to PIV.
2. Wave propagation over a submerged plate (installed at 6 cm below the still water level) being modeled in a 30 cm wide wave flume for a wave height H = 4 cm, a wave period T = 1 s, and a water depth of 30 cm (images taken from Bung et al. 2008); the water is again seeded with particles, and images are taken with a high-speed camera with only 256 x 256 px resolution at 500 fps; OF is compared to numerical results from a Large Eddy Simulation.
3. Slightly aerated flow over a stepped spillway with 50 cm width, 6 cm step height, 1V:2H slope, and a specific discharge q = 0.07 m^2/s; the high-speed video is captured at 732 fps and a resolution of 1920 x 1200 px on step 5, which was found to be the inception point of surface self-aeration by Bung (2011a) (the same setup has been previously used in Bung and Valero (2016) for OF determination for fully aerated flow); water is not seeded in this experiment and, hence, OF is performed on transported air bubbles; OF is compared to BIV results.

MatPIV in its latest version 1.61 is employed for calculation of PIV- and BIV-based velocity fields. MatPIV (Sveen 2004) is another open-source toolbox for MATLAB®, which applies a classical PIV technique allowing variation of several parameter settings, e.g. interrogation window size, window overlap, and different filtering methods for smoothing of the velocity field. The reader may note that the studies were conducted by use of simple halogen spotlights being installed in front of the inspection window and above the flumes. It is acknowledged that the presented results are likely affected by sidewall effects as the applied illumination does not allow to define a thin measuring plane as laser sheets usually do. Thus, particles and bubbles near the sidewall are taken into account as well as those in the rear. This fact may also lead to some distortion affecting the results. Moreover, it is pointed out that 3D flow fields are reduced to 2D for all methods.

3. RESULTS

3.1. Dam Break Flow

This case is analyzed with both methods, OF and PIV using MatPIV. As PIV is a well-established method in hydraulic engineering, this technique is applied to compare and assess the OF capabilities. The PIV calculations are performed with quadratic interrogation windows and 50% overlap. Although MatPIV generally includes several filter options to improve results, all calculations are carried out without any filtering and smoothing.

Figure 1 illustrates the first high-speed image, which was recorded at t = 0.50 s after the gate release. In physical scale, the image is roughly 90 cm wide, yielding a pixel density of ~14 px/cm. In combination with the subsequent frame being recorded 1/900 s later, velocities are determined by both imaging techniques and compared to velocity profiles that were visually extracted from the images. For this purpose, four sections of the images were selected with a width of 16 px each, namely at x = -7 cm (section 1), x = 8 cm (section 2), x = 23 cm (section 3), and x = 38 cm (section 4) where the gate axis defines the zero position x = 0 cm (see Fig. 1). Particles within these sections were tracked by eye from one frame to the next, and their displacements were noted. Due to the high

density of particles, displacement data were obtained with an average distance of roughly 4 px along the water column (e.g. 38 data points were obtained in section 3, where the water depth was given by 160 px).

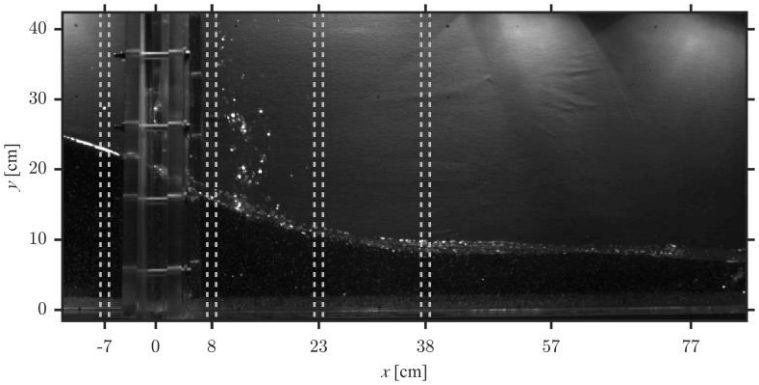

Figure 1. High-speed frame at t = 0.50 s after gate opening (from Oertel and Bung, 2012)

The main parameters influencing the quality of calculated results within the two image processing techniques are given by the number of iterations in each warping step for OF and the interrogation window size for PIV. In order to quantify these influences, both parameters have been systematically varied and the resulting mean error defined by

$$meanerror = \frac{1}{n}\sum_{i}^{n}\frac{vel_{im,i} - vel_{vis,i}}{vel_{vis,i}} \tag{5}$$

has been determined. In Eq. (5) n is the total number of visually detected data points in a section, $vel_{vis,i}$ is the i^{th} visually determined velocity magnitude and $vel_{im,i}$ the velocity magnitude in the same elevation from each imaging technique. Using a median filter of size 12 x 12 px for smoothing of the dense data in OF, the mean errors in Fig. 2 were obtained. PIV calculations were run using a multiple approach with three different decreasing interrogation window sizes, i.e. the final pass was run with half of the initial window size.

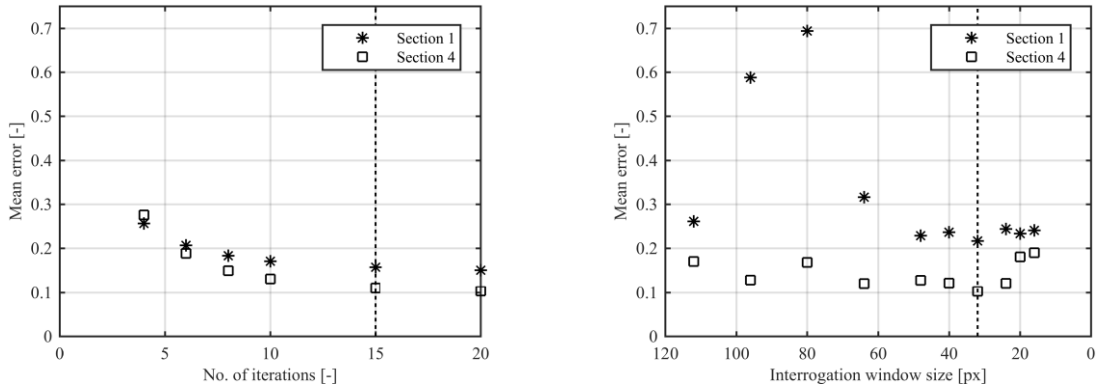

Figure 2. Sensitivity of image processing techniques to parameter settings, exemplarily for section 1 and 4; dashed lines for selected settings; left: number of iterations (OF), right: interrogation window size (PIV).

Obviously, both imaging methods produce results of similar accuracy if settings are properly chosen. In section 1, where there are relatively low velocities, the mean error in PIV is about 0.217 for an initial interrogation window size of 32 x 32 px while it is 0.157 for 15 iterations in OF. The reader may note that the mean error decreases in negligible order for a higher number of iterations. In section 4, with higher flow velocities, both techniques reach the same accuracy with a mean error of 0.103 for PIV again using a 32 x 32 px initial window and 0.110 for OF using 15 iterations. While a clear decreasing trend of the mean error is found in OF with increasing number of iterations, a critical interrogation window size is found in PIV giving the highest accuracy. This fact may be explained by

particle displacements being larger than the final interrogation window size when smaller windows are considered. Particles are then no longer available in the second frame for cross-correlation.

Figure 3 shows the resulting velocity magnitude profiles for sections 1 to 4 using the above detected optimal settings, i.e. 15 iterations for OF and 32 x 32 px for PIV. In order to avoid spurious velocities above the water surface line due to local brightness patterns (Fig. 1), dry areas have been masked before processing. PIV and visual data have been smoothed with a moving average filter in order to get a comparable filtering as it was used for OF. It is found that the velocity data from both techniques compare fairly well. For sections 2 and 4, the differences are very small while for section 1 and 3, some deviation is noted, namely better prediction by OF in section 1 and by PIV in section 3. In any case, PIV supports the calculated shape of the velocity profile. It is observed that both PIV and OF show a lack in accuracy close to the boundaries where an unnatural decrease of velocity is obtained. This decrease may be explained by the smoothing in OF and the overlap of the interrogation window to non-moving areas (masking may support avoiding this error).

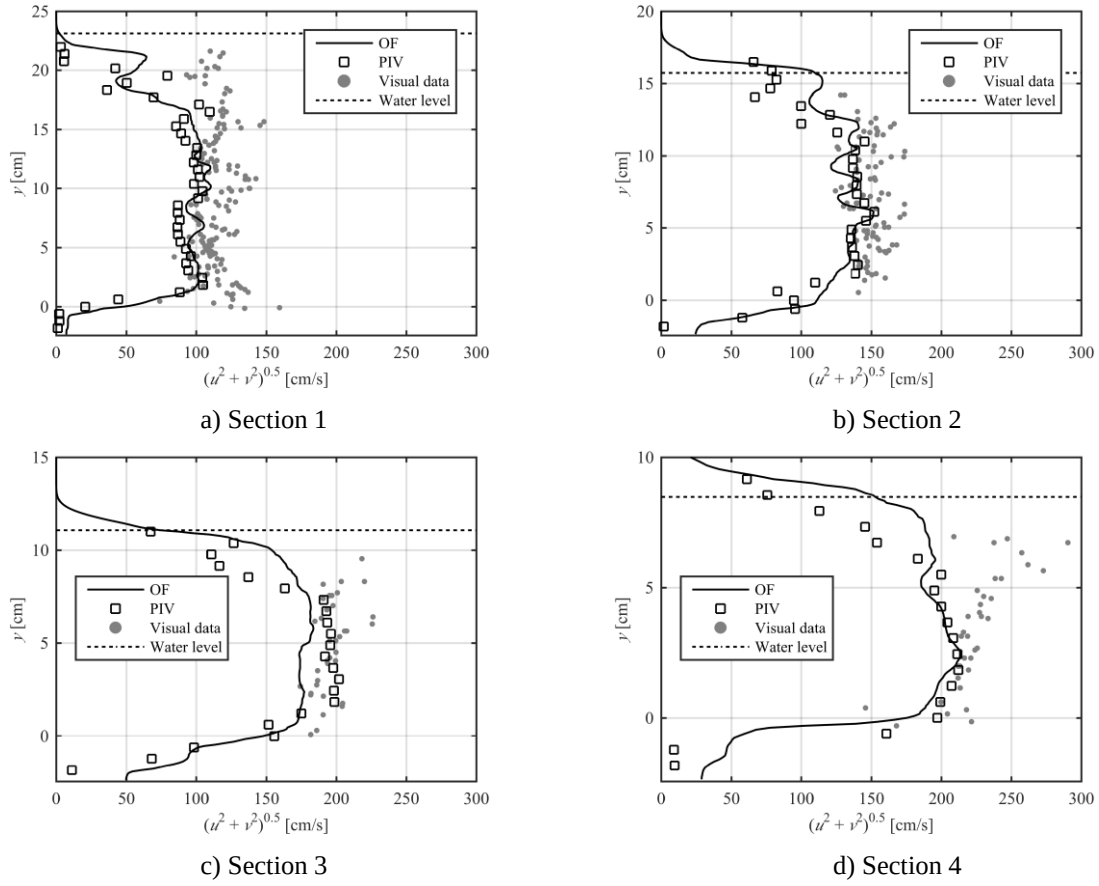

Figure 3. Velocity magnitude profiles extracted from image processing techniques in comparison to visually determined velocities for four sections (OF data obtained by 15 iterations, PIV data obtained with an interrogation window of 32 x 32 px, note the different scaling of the *y*-axis)

Figure 4 presents the complete velocity magnitude fields. It must be noted that, for better readability, the OF result displays only every 25th vector, while the PIV result includes every 3rd vector to ease comparison of both plots. In the OF result, some spurious vectors appear in the air region due to fluctuation in the illumination. Those vectors can be eliminated by some image pre-processing, which was not done in the present study. The PIV result shows less spurious vectors. Processing times for OF (Table 1) and PIV (Table 2) are given below. The calculations were performed on a Laptop with a 3.1 GHz Dual-Core Intel i7 processor, 16 GB RAM, and a SSD hard disk. Accordingly, the calculation time in OF takes 28 times the time needed for PIV using the optimal settings (highlighted in gray). However, the absolute time is still acceptable with ~3 minutes regarding the much

higher information density obtained by OF, i.e. 65 times more velocity vectors. Depending on the purpose of a given study, this denser information may be of benefit, e.g. for a vortex flow. However, it is pointed out that the performed averaging (median filter of size 12 x 12 px) is relatively time-consuming. Comparative processing of this case without filtering took only 123.0 s.

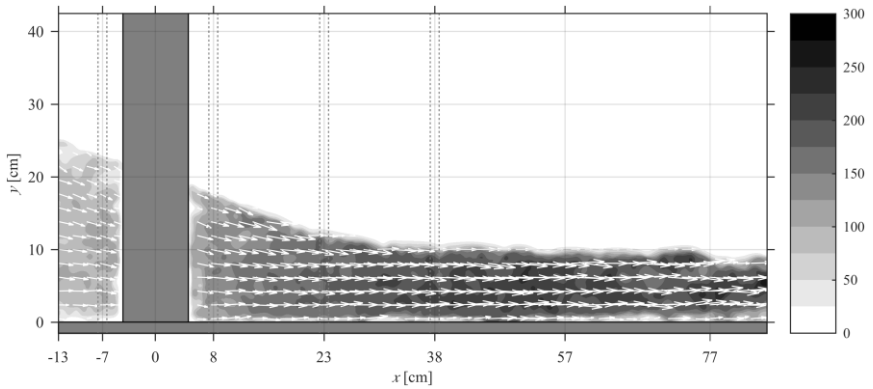

a) Optical Flow for 15 iterations (every 25th vector displayed)

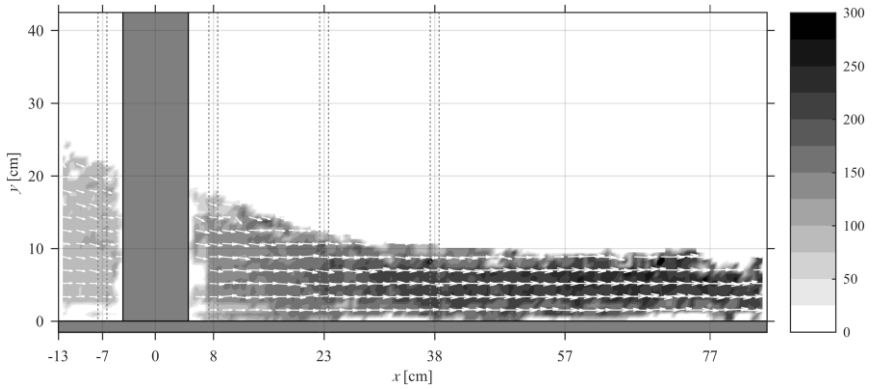

b) Particle Image Velocimetry for 32 x 32 px initial interrogation window size (every 3rd vector displayed)

Figure 4. Resulting velocity magnitude fields (in cm/s)

Table 1. Calculation time for different iteration numbers in OF method (2 to 20 iterations) and resulting size of the velocity field

Method	**OF 2**	**OF 4**	**Of 6**	**OF 8**	**OF 10**	**OF 15**	**OF 20**
Time (s)	28.8	51.8	75.3	99.8	133.4	183.7	239.9
VF size (px x px)	1280 x 576						

Table 2. Calculation time for different initial interrogation window size in PIV method (112 x 112 px to 16 x 16 px) and resulting size of the velocity field (the final calculation pass used 50 % of the given interrogation window size)

Method	**PIV 112**	**PIV 96**	**PIV 80**	**PIV 64**	**PIV 48**	**PIV 40**	**PIV 32**	**PIV 24**	**PIV 20**	**PIV 16**
Time (s)	3.2	4.3	5.5	3.9	6.1	8.1	6.5	11.2	15.8	19.0
VF size (px x px)	19 x 44	23 x 52	27 x 63	35 x 79	47 x 105	56 x 127	71 x 159	95 x 212	114 x 255	143 x 319

3.2. Wave Breaking at Artificial Reef

In order to evaluate the performance of the OF method, a regular wave propagating over a submerged plate is investigated in the following. Figure 5 shows the images taken from the high-speed video at six instants over the wave period of 1 s (left column) as well as the results from OF (center column) in comparison with numerical results from a 2D LES simulation obtained by FLOW-3D (right column).

The field of view is limited to the rear end of the submerged plate. The high-speed images cover a range of ~23 x 23 cm with a resolution of 256 x 256 px. The pixel density, i.e. ~11 px/cm, is thus comparable to the previous test case and the same mean averaging filter size of 12 x 12 px is chosen. The time $t = 0$ s was chosen as the moment where the backflow above the plate is just about to set in. Thus, the water is in rest in this moment, and only a small vortex being generated at the end of a wave cycle is still present. A mesh with 5 mm cell size was chosen to resolve the directly simulated large vortices in the LES model.

The flow field in this test case is characterized by several small-scale vortex structures being transported around the plate as well as some aeration after the wave breaking. Generally, the flow velocities, which are obtained by Optical Flow, are in good agreement with the numerical solution. The very complex flow fields consisting of forwards and backwards directed particle displacements are well represented. Moreover, the small vortices at the end of the plate are in good agreement regarding their size and location. It has to be noted that a relatively small interrogation window size would be required to detect these vortex structures with a PIV technique. The OF calculation time for each frame pair was about 10 s on the same computer as in the test case 1 due to the low image resolution. It was found again that the OF method is sensitive to illumination changes leading to high number of spurious vectors above the water surface. For a better readability and comparability, these regions have been masked in the OF result plots.

3.3. Aerated Stepped Spillway Flow

In this section, OF application to slightly aerated flows (with a mean air concentration of 20 %) is tested. Therefore, a high-speed recording of a stepped spillway flow is used. The video is captured with a frame rate of 732 fps and a full resolution of 1920 x 1200 px. Two frames were extracted from the video and rotated by 26.6° to align the pseudo-bottom (connecting the step edges) with the horizontal. The images were cropped to the field of interest, i.e. one single step, yielding an image size of 1270 x 1100 px (Fig. 6a). As the investigated step represents the inception point of self-aeration, clear water is found at the upstream end of the step while flow at the downstream end is aerated. The pixel density is about 90 px/cm in this study, much higher than in the previous cases.

A simple OF estimation as it was performed in the first two cases was found to not provide useful results. For this reason, the image pyramid technique is considered, which is an incremental multi-resolution method. This method is used to apply a single filter to a set of images instead of using different filters to a single image (Adelson et al. 1984, Burt and Adelson1983). Herein, the original image size is reduced by a specified factor yielding a blurred (low-pass filtered) copy of the image when upscaled to its original size. Repeating this step several times, a set of images of different sizes are obtained, forming a pyramid when illustrated above each other. In fact, this pyramid is the spatial-frequency domain of the image. Each level is downsampled from its nearest finer level. The optical flow is estimated at a coarse level in a first step. The coarse scale displacement is then used to correct the sequence at the next finer level (warping) (Sun et al. 2010). The total displacement is then the sum of all increments, resulting in higher accuracy for large displacements (Bruhn et al. 2005).

Naturally, the image pyramid technique is even more time-consuming than the basic Horn and Schunck scheme. For the given sequence of the stepped spillway, the total calculation time was 817.2 s using five pyramid levels with a downsampling factor of 2.5, which yields a minimum image size of 13 x 11 px. The results are illustrated in Fig. 6b in comparison to data from a conductivity probe. This data was gathered by Bung (2011a) in the centreline of a 30 cm wide flume with identical step height, slope and specific discharge. Moreover, an exemplary BIV result is included. For BIV, an interrogation window size of 32 x 32 px with 75 % overlap was applied. The results show that the OF method can give valuable results even in aerated flows, which is known to be difficult by imaging techniques

(Bung 2011b). While BIV commonly tends to provide too low velocities (Bung and Valero 2015), OF is a more robust method in aerated flow analysis.

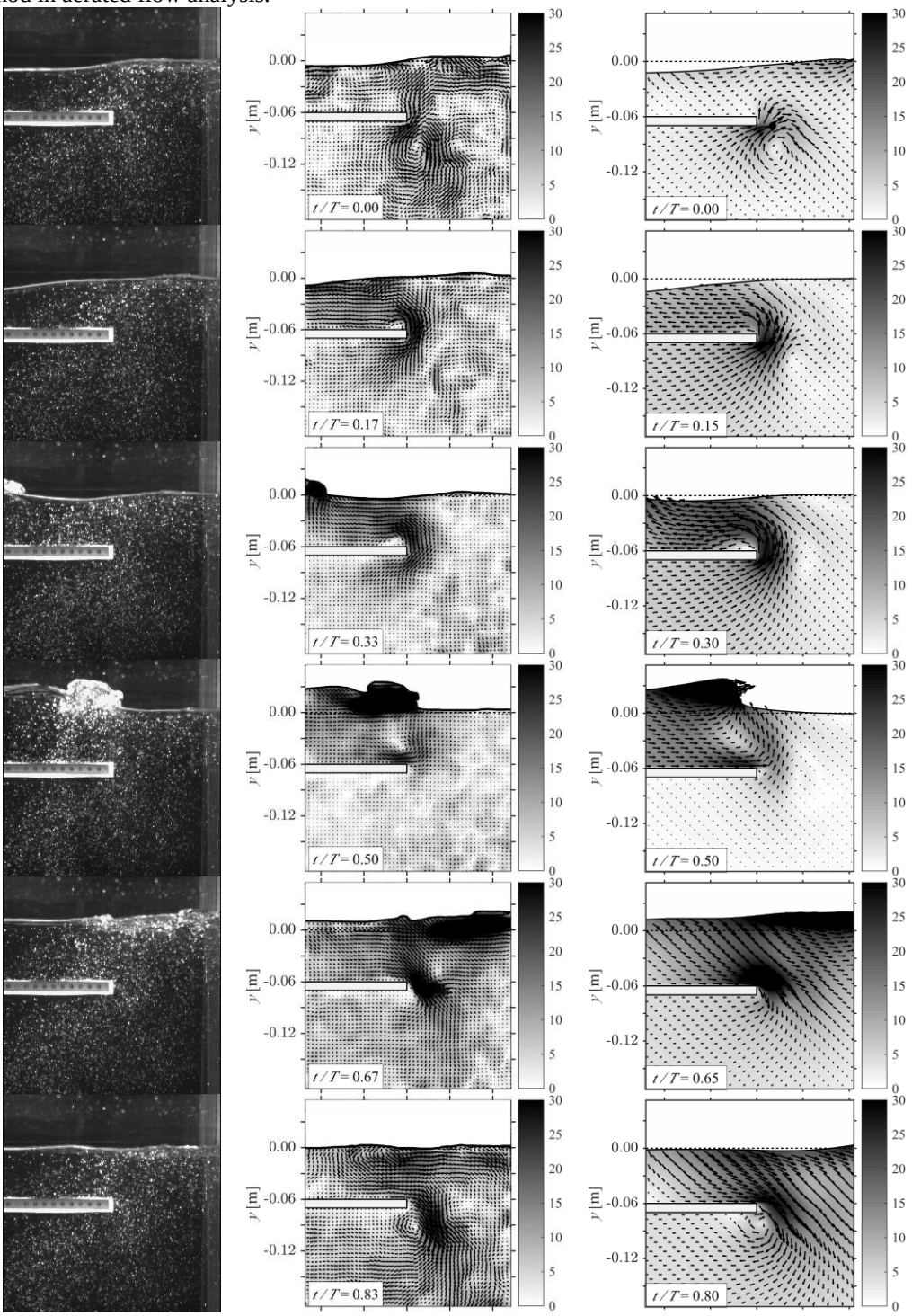

Figure 5. Velocity magnitude fields over one wave period (top to bottom) at the rear end of the submerged plate (in cm/s) obtained from high-speed video frames (left, from Bung et al. 2008) using OF method (center) in comparison to LES simulation (right), note that spurious vectors in OF results have been masked above the free surface

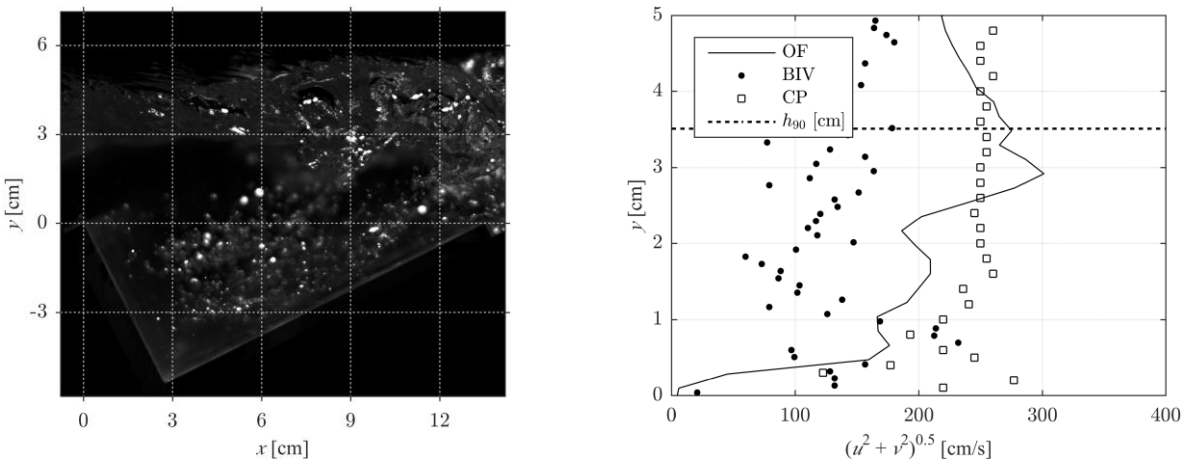

a) High-speed frame captured at step 5, i.e. the inception point of self-aeration with C_{mean} = 20 %, flow direction from left to right

b) Velocity profile obtained by OF method compared to BIV and conductivity probe data (CP) from the centreline (h_{90} is the elevation with a time-averaged air concentration of 90 %)

Figure 6. Optical Flow method in slightly aerated stepped spillway flows

3.4. Conclusions

It was shown that the Optical Flow method is fully capable to determine 2D velocity fields in hydraulic structure models. When choosing a global method, e.g. the Horn and Schunck method used in the present paper, a dense velocity field is obtained. Velocity information is then given for every pixel. The calculation time is much longer compared to a classical PIV calculation. However, PIV results are typically of lower resolution and do not allow the determination of such dense velocity fields, except with additional interpolation. The calculation time for OF is still bearable on modern computers and may be reasonable when detection of small-scale rotational flow structures is of interest.

The OF method was successfully applied to seeded and aerated flows although OF, as a differential approach, should be better suitable for continuous objects than for small particles. Moreover, OF is much more sensitive to local illumination changes as it is a differential approach compared to PIV as an integral approach.

In case of aerated flows, calibration of the data is still recommended. Particularly, application of an image pyramid technique helps to improve the results. Application to other types of aerated flows is planned for future research. A detailed benchmark with direct velocity measurements near the wall using an intrusive probe may help in assessing accuracy of the presented method.

References

Adelson, E., Anderson, C. H., Bergen, J. R., Burt, P. J., and Ogden, J. M. (1984). "Pyramid methods in image processing." RCA Engineer, 29(6), 33-41.

Adrian, R.J., and Westerweel, J. (2011). Particle Image Velocimetry, Cambridge University Press, Cambridge.

ASCE (2000). Hydraulic modeling - concepts and practice, ASCE manuals and reports on engineering practice, No. 97, Reston.

Bruhn, A., Weickert, J., and Schnörr, C. (2005). "Lucas/Kanade meets Horn/Schunck: Combining local and global optic flow methods." *International Journal of Computer Vision*, 61(3), 211-231.

Bung, D.B. (2011a). "Developing flow in skimming flow regime on embankment stepped spillways." *Journal of Hydraulic Research*, 49(5), 639-648.

Bung, D.B. (2011b). “Non-intrusive measuring of air-water flow properties in self-aerated stepped spillway flow.” 34th IAHR World Congress, Brisbane, 2380-2387.

Bung, D.B., and Valero, D. (2015). “Image processing for Bubble Image Velocimetry in self-aerated flows.” *36th IAHR World Congress*, Den Haag.

Bung, D.B., and Valero, D. (2016). “Optical flow estimation in aerated flows.” *Journal of Hydraulic Research* (accepted paper)

Bung, D.B., Hildebrandt, A., Oertel, M., Schlenkhoff, A., and Schlurmann, T. (2008). “Bore propagation over a submerged horizontal plate by physical and numerical simulation.” *31st International Conference on Coastal Engineering (ICCE)*, Hamburg.

Burt, P. J., & Adelson, E. H. (1983). “The Laplacian pyramid as a compact image code.” *IEEE Transactions on Communications*, 31(4), 532-540.

Corpetti, T., Heitz, D., Arroyo, G., Memin, E., and Santa-Cruz, A. (2006). “Fluid experimental flow estimation based on an optical-flow scheme.” *Experiments in Fluids*, 40(1), 80-97.

Felder, S., and Chanson, H. (2015). “Phase-detection probe measurements in high-velocity free-surface flows including a discussion of key sampling parameters.” *Experimental Thermal and Fluid Science*, 61, 66-78.

Fortun, D., Bouthemy, P., and Kervrann, C. (2015). “Optical flow modeling and computation: A survey.” *Computer Vision and Image Understanding*, 134, 1-21.

Horn, B.K.P., and Schunck, B.G. (1981). “Determining optical flow.” *Artificial Intelligence*, 17, 185-203.

Leandro, J., Bung, D.B., and Carvalho, R. (2014). “Measuring void fraction and velocity fields of a stepped spillway for skimming flow using non-intrusive methods.” *Experiments in Fluids*, 55(5).

Liu, T., Merat, A., Makhmalbaf, M.H.M., Fajardo, C., and Merati, P. (2015). “Comparison between optical flow and cross-correlation methods for extraction of velocity fields from particle images.” *Experiments in Fluids*, 56(8).

Liu, T., and Shen, L. (2008). “Fluid flow and optical flow.” *Journal of Fluid Mechanics*, 614, 253–291.

Lucas, B.D., and Kanade, T. (1981). “An iterative image registration technique with an application to stereo vision.” *Proceedings of imaging understanding workshop*, 121-130.

Oertel, M., and Bung, D.B. (2012). “Initial stage of two-dimensional dam-break waves: Laboratory vs. VOF.” *Journal of Hydraulic Research*, 50(1), 89-97.

Ryu, Y., Chang, K.-A., and Lim, H.-J. (2005). “Use of bubble image velocimetry for measurement of plunging wave impinging on structure and associated greenwater.” *Meas. Sci. Technol*., 16 (10), 1945-1953.

Sun, D., Roth, S., & Black, M. J. (2010). “Secrets of optical flow estimation and their principles.” *IEEE conf. on computer vision and pattern recognition* (cvpr).

Sveen (2004). “An introduction to MatPIV v.1.6.1.” *Department of Mathematics, Mechanics and applied Mathematics, University of Oslo*.